

## Supporting Information

### Nitrogen and Oxygen co-doped 3D nanoporous duct-like graphene@carbon nano-cages hybrid films for high-performance multi-style supercapacitors

*Kaiqiang Qin, Liping Wang, Ning Wang, Jiajun Li, Naiqin Zhao\*, Chunsheng Shi, Chunnian He, Fang He, Liying Ma, Enzuo Liu\**

The specific capacitance of the electrode material ( $C_s$ , F g<sup>-1</sup>) tested in two-electrode system was calculated from GCD discharge curve:

$$C_s = \frac{2 \times I \times \Delta t}{\Delta V \times m} \quad (1)$$

Where  $I$  is the constant current in discharging,  $m$  is the mass of active material on one electrode,  $\Delta t$  is the discharge time, and  $\Delta V$  is the voltage change during discharge.

Energy density ( $E$ , Wh Kg<sup>-1</sup>) of the cell was calculated by:

$$E = \frac{C_s \times \Delta V^2}{2 \times 4 \times 3.6} \quad (2)$$

Average power density ( $P$ , W Kg<sup>-1</sup>) of the cell was obtained by:

$$P = \frac{E \times 3600}{\Delta t} \quad (3)$$

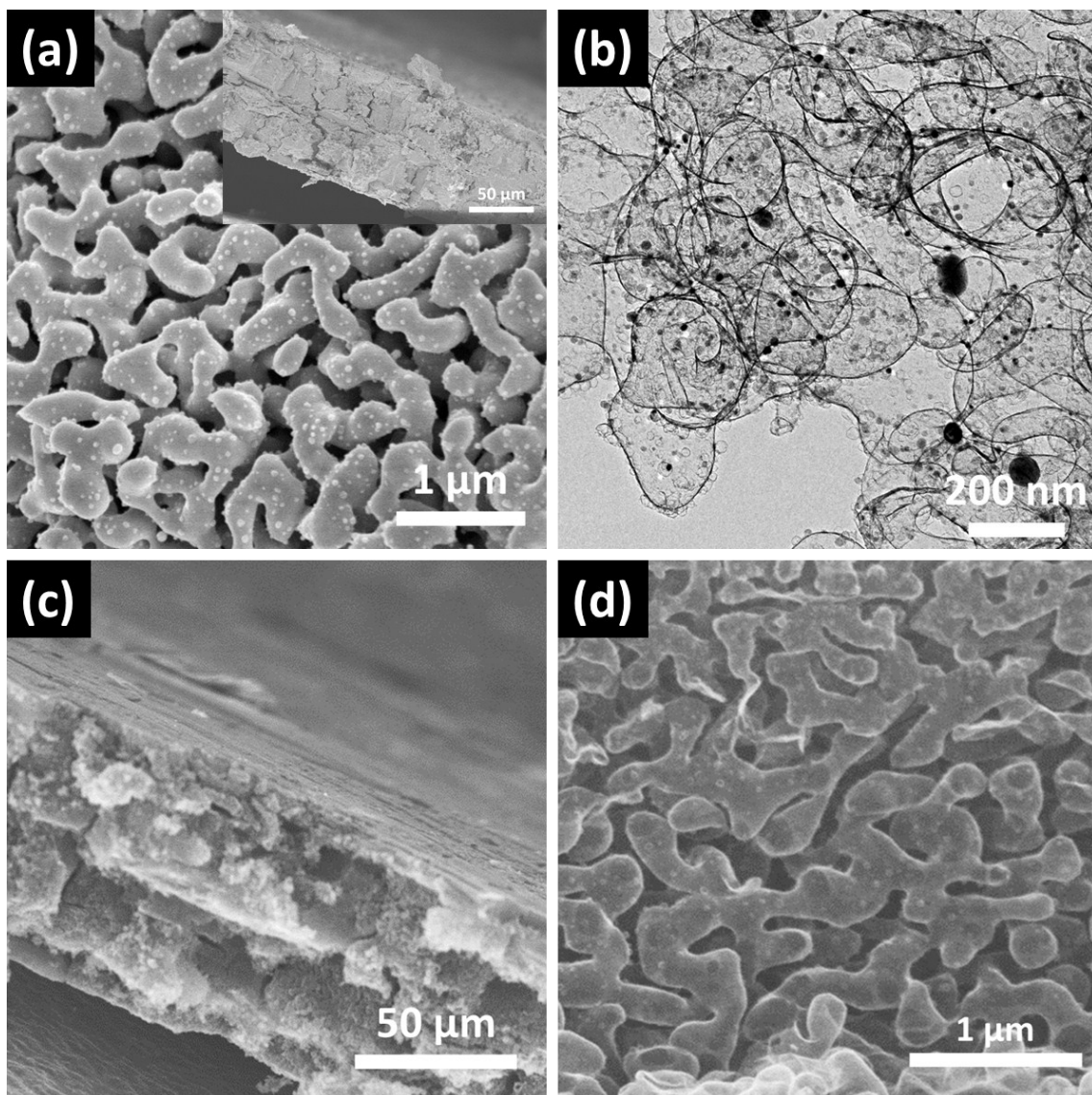


**Figure S1.** (a) SEM image of NPC/N-3DG@CNCs film. The inset shows the thickness of NPC/N-3DG@CNCs film. (b) TEM image of N-3DG@CNCs without further treated by  $\text{HNO}_3$ . (c,d) SEM images of NO-3DG@CNCs film.

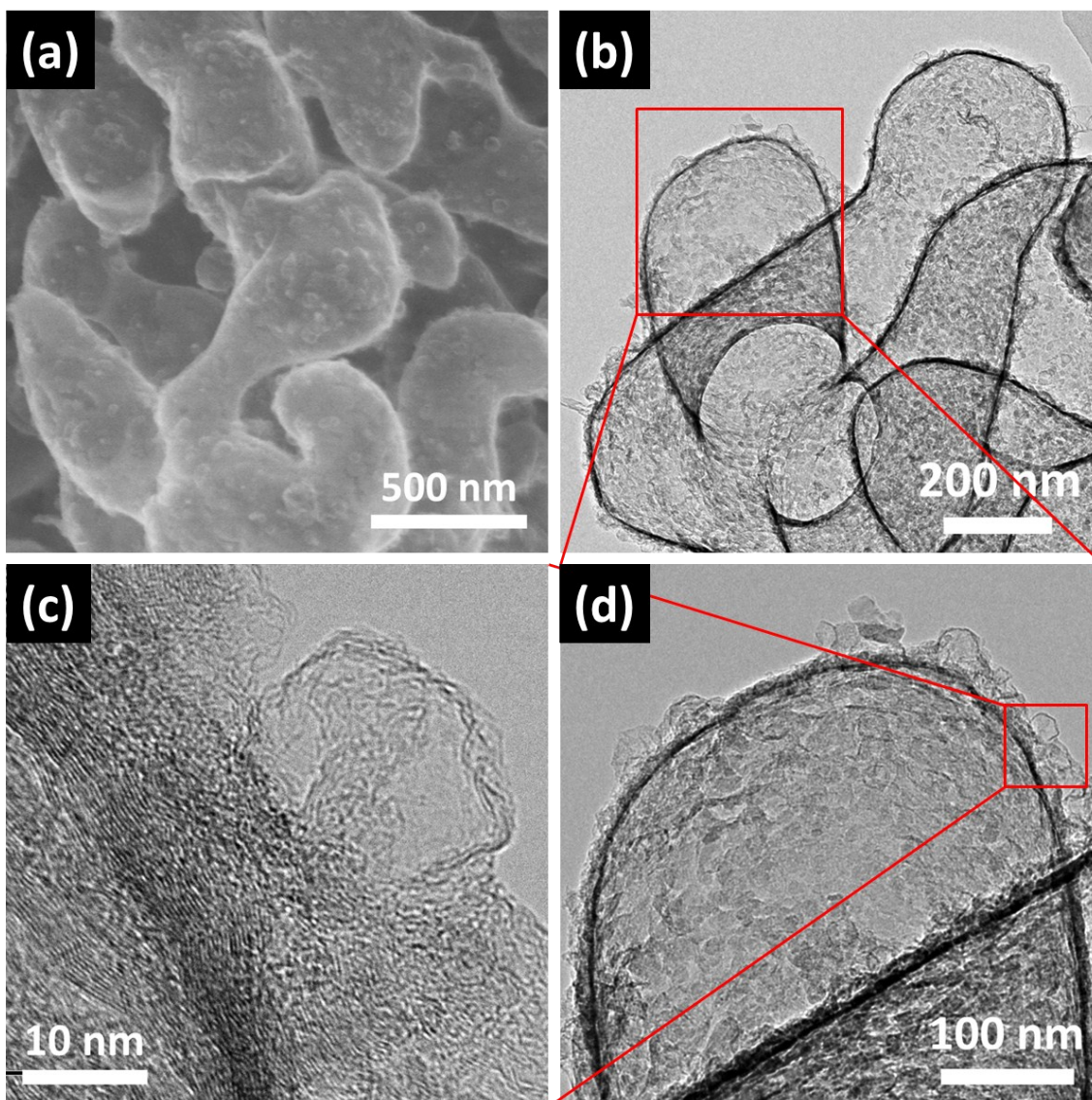


**Figure S2.** (a) SEM image of the O-3DG@CNCs film. (b-d) TEM images of O-3DG@CNCs film.

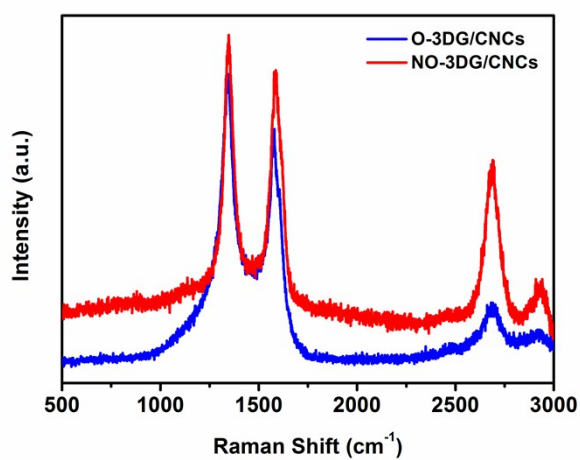


**Figure S3.** Raman analysis of the O-3DG@CNCs and NO-3DG@CNCs.

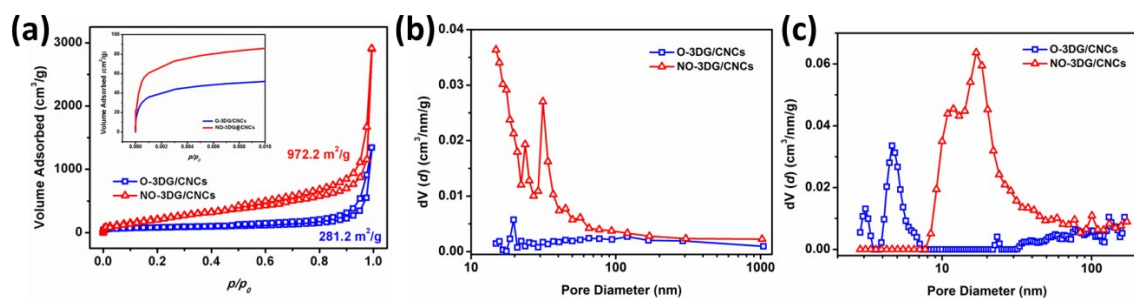


**Figure S4.** (a) Nitrogen adsorption-desorption isotherm of O-3DG@CNCs and NO-3DG@CNCs. The inset shows the BET curves in the sections of  $p/p_0 < 0.01$ . (b and c) BJH and DFT pore size distribution of O-3DG@CNCs and NO-3DG@CNCs.

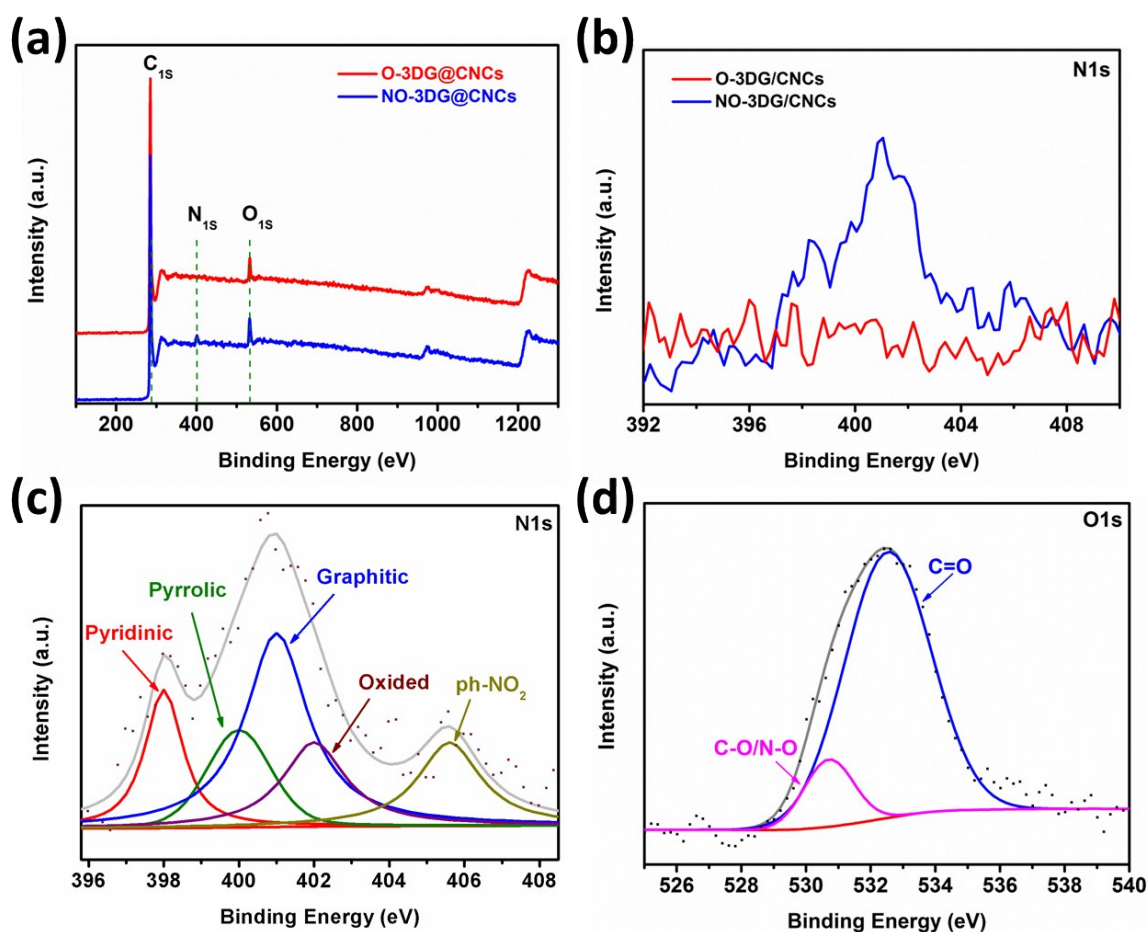


**Figure S5.** (a) XPS spectra of the surface chemical composition of the as-prepared O-3DG@CNCs and NO-3DG@CNCs. (b) The comparison of N<sub>1s</sub> XPS spectra between O-3DG@CNCs and NO-3DG@CNCs. (c and d) N<sub>1s</sub> and O<sub>1s</sub> XPS spectra of NO-3DG@CNCs.

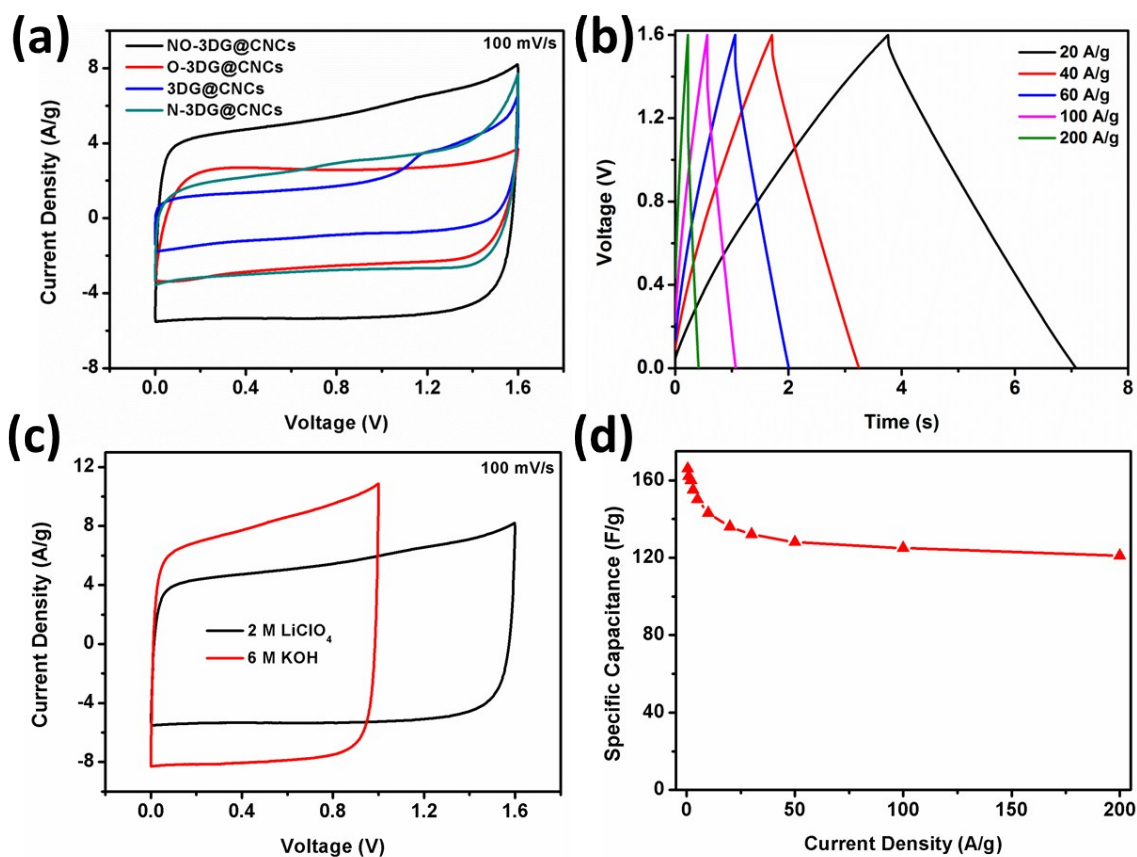


**Figure S6.** (a) CV curves of NO-3DG@CNCs, O-3DG@CNCs, 3DG@CNCs and N-3DG@CNCs based SSCs at a scan rate of 100 mV/s. (b) Galvanostatic charging/discharging curves of NO-3DG@CNCs based SSCs at various current densities ranging from 20 to 200 A/g. (c) CV curves of NO-3DG@CNCs electrode in 6 M KOH solution and 2 M LiClO<sub>4</sub> solution at a scan rate of 100 mV/s at different voltage windows. (d) The specific capacitance of NO-3DG@CNCs at different current densities in 6 M KOH solution.

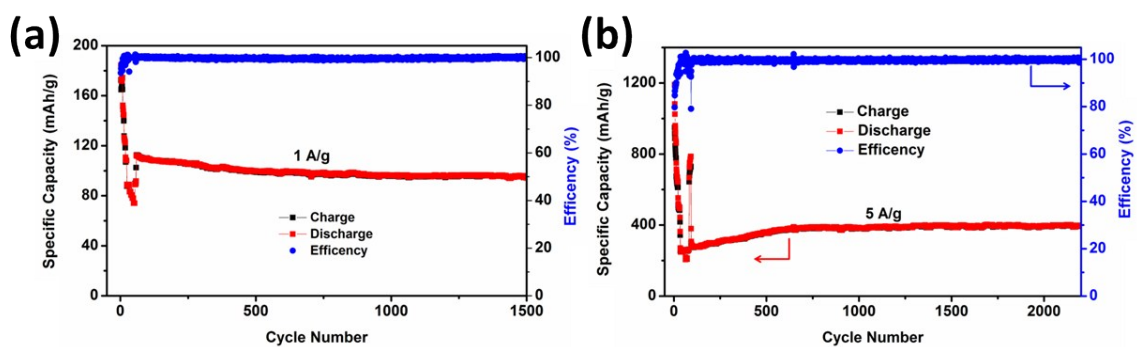


**Figure S7.** Cycle behaviors and coulombic efficiency of NO-3DG@CNCs as (a) cathode and (b) anode.

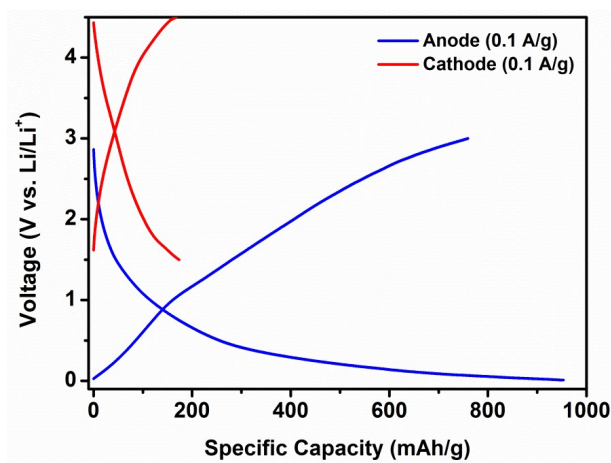


**Figure S8.** Charge-discharge curves of NO-3DG@CNCs as cathodes (1.5-4.5 V) and as anodes (0.01-3.0 V) in half-cell with Li foil as the counter and reference electrode (0.1 A/g).

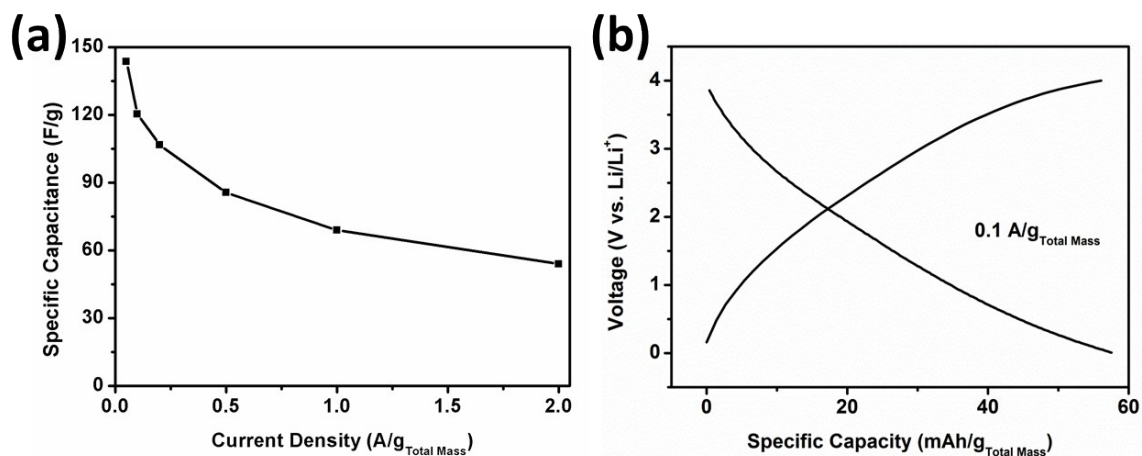


**Figure S9.** (a) Specific capacity of NO-3DG@CNCs based LICs as a function of current density. (b) Charge-discharge curves of the NO-3DG@CNCs based LICs (0.1 A/g).